

## A COMPARISON BETWEEN THIN-FILM TRANSISTORS DEPOSITED BY HOT-WIRE CHEMICAL VAPOR DEPOSITION AND PECVD

Meysam Zarchi\*, Shahrokh Ahangarani

*Advanced Materials & Renewable Energies Department, Iranian Research  
Organization for Science and Technology, Tehran, Iran*

*Received 20.08.2014*

*Accepted 30.09.2014*

### Abstract

The effect of new growth techniques on the mobility and stability of amorphous silicon (a-Si:H) thin film transistors (TFTs) has been studied. It was suggested that the key parameter controlling the field-effect mobility and stability is the intrinsic stress in the a-Si:H layer. Amorphous and microcrystalline silicon films were deposited by radiofrequency plasma enhanced chemical vapor deposition (RF-PECVD) and hot-wire chemical vapor deposition (HW-CVD) at 100 °C and 25 °C. Structural properties of these films were measured by Raman Spectroscopy. Electronic properties were measured by dark conductivity,  $\sigma_d$ , and photoconductivity,  $\sigma_{ph}$ . For amorphous silicon films deposited by RF-PECVD on PET, photosensitivity's of  $>10^5$  were obtained at both 100 °C and 25 °C. For amorphous silicon films deposited by HW-CVD, a photosensitivity of  $>10^5$  was obtained at 100 °C. Microcrystalline silicon films deposited by HW-CVD at 95% hydrogen dilution show  $\sigma_{ph} \sim 10^{-4} \Omega^{-1}cm^{-1}$ , while maintaining a photosensitivity of  $\sim 10^2$  at both 100 °C and 25 °C. Microcrystalline silicon films with a large crystalline fraction ( $> 50\%$ ) can be deposited by HW-CVD all the way down to room temperature.

*Keyword: Thin Film Transistors, PECVD, Deposited, Silicon Films, Stress*

### Introduction

Amorphous silicon (a-Si:H) thin film transistors (TFT), commonly deposited by plasma enhanced chemical vapor deposition (PECVD) at 13.56 MHz, are widely used as pixel-switching devices in large area electronics. The low field-effect mobility ( $< 1 \text{ cm}^2/V \text{ s}$ ) and the limited stability under gate bias stress, due to defect creation in the a-Si:H, complicates the utilization in applications where high performance is demanded, such as OLED displays and column/row-addressing circuitry. While the low mobility is attributed to the inherent condition of a-Si:H, the microscopic specifics of the defect-creation mechanism (Staebler–Wronski effect) are still elusive.

---

\* Corresponding autor: M. Zarchi, sky\_man1983@yahoo.com

TFTs incorporating PECVD a-Si:H with high compressive stress exhibited a poor stability [1]. This was explained with a high fraction of short (compressed) Si-Si bonds, of which the energy levels are located in the valence-band tail, which tend to break under charge accumulation, thus forming dangling-bond defects. This process is thermally activated with an exponential distribution of barrier heights.

Since ‘device-quality’ a-Si:H usually has high compressive stress, combining a high field-effect mobility with a high TFT stability seems to be contradictory. Therefore, other deposition techniques, such as very-high frequency (VHF) RF-CVD [2] and hot-wire (HW) CVD [3] have been used for TFT deposition. It could be shown that TFTs with a high stability, maintaining a high mobility, are feasible [4]. We now present a comprehensive study of the stability and mobility of VHF and hot-wire TFTs.

### Experimental Procedures

For HW deposition, a single tungsten filament coil of 0.5 mm diameter and approximately 7 cm total length was placed 5 cm from the substrate and was resistively heated with a DC power supply.

The filament temperature was measured with an optical pyrometer (Tfil ~ 2500 °C) and the pressure was kept constant at 20 mTorr. For the RF deposition, the inter-electrode distance was 3 cm, the density of RF power used was 50 mW/cm<sup>2</sup> (in all experiments, but at the room temperature depositions where RF power was 100 mW/cm<sup>2</sup>, whereas the pressure was 100 mTorr). For both the HW and RF depositions, the sum of gas fluxes was kept at around 10 cm<sup>3</sup>/min, except for the higher dilutions where it was necessary to increase the flux so that the SiH<sub>4</sub> flux was not less than 0.5 cm<sup>3</sup>/min, which was the lower limit for the silane mass flow controller. Films were deposited on Corning 7059 glass and polyethylene terephthalate (PET) [7]. The PET was covered by a 200 nm thick SiN<sub>x</sub> passivation layer. Raman spectra were measured in the backscattering geometry using a Raman microprobe. The power of the incident beam was set below 50 mW to avoid thermally induced crystallization [8-10].

### Results

Table 1 summarizes the measured properties of selected films deposited on substrate.

Table 1. Properties of films deposited on substrate.

CVD techn	RF-PECVD (a-Si:H)						HW (a-Si:H)					
	25 °C			100 °C			25 °C			100 °C		
Temp												
Sample	S1493	S1518	S1489	S1486	S1520	S1487	S1515	S1494	S1519	S1501	S1488	S1498
H <sub>2</sub> (%)	98	99	99	96	98	98	80	80	90	60	60	90
d (μm)	0.1	0.3	0.1	0.1	0.3	0.1	0.3	0.1	0.3	1.0	0.1	0.1
σ <sub>a</sub> (Ω <sup>-1</sup> cm <sup>-1</sup> )	1.9 x 10 <sup>-11</sup>	6.3 x 10 <sup>-9</sup>	1.1 x 10 <sup>-9</sup>	1.0 x 10 <sup>-10</sup>	3.8 x 10 <sup>-6</sup>	1.4 x 10 <sup>-11</sup>	6.9 x 10 <sup>-10</sup>	3.8 x 10 <sup>-10</sup>	2.0 x 10 <sup>-7</sup>	2.4 x 10 <sup>-11</sup>	1.3 x 10 <sup>-10</sup>	2.5 x 10 <sup>-6</sup>
E <sub>a</sub> (eV)	0.43	0.66	0.57	0.87	0.4	0.9	0.74	0.65	0.68	0.55	0.85	0.56
σ <sub>ph</sub> (Ω <sup>-1</sup> cm <sup>-1</sup> )	1.1 x 10 <sup>-7</sup>	3.5 x 10 <sup>-9</sup>	3.7 x 10 <sup>-6</sup>	5.0 x 10 <sup>-6</sup>	2.4 x 10 <sup>-8</sup>	7.6 x 10 <sup>-6</sup>	2.0 x 10 <sup>-7</sup>	2.9 x 10 <sup>-7</sup>	6.2 x 10 <sup>-8</sup>	3.4 x 10 <sup>-6</sup>	2.2 x 10 <sup>-5</sup>	1.5 x 10 <sup>-7</sup>

where:  $d$ - film thickness,  $\sigma_d$ - dark conductivity,  $\Omega^{-1} \text{ cm}^{-1}$  and  $\sigma_{ph}$ -photoconductivity,  $\Omega^{-1} \text{ cm}^{-1}$

The Raman spectra of films deposited by RF-PECVD on PET (Fig. 1a and Fig. 1b) show the dependence of the crystalline fraction on film thickness of samples deposited at substrate temperatures of 100 °C and 25 °C.

When the film thickness increases from 100 to 300 nm, the crystalline fraction increases from 16 to 40% for the film deposited at  $T_{sub}=25$  °C and 99%  $\text{H}_2$  dilution, and from 12 to 55% for the film deposited at  $T_{sub}=100$  °C and 98%  $\text{H}_2$  dilution. The crystalline fractions of the 300 nm RF films on PET approach those of the corresponding films deposited on glass, i.e. 42% for the 25 °C and 58 % for the 100 °C sample. The same effect can be observed in the case of the HW film deposited at 25 °C on PET using 90% hydrogen dilution (Fig. 1c).

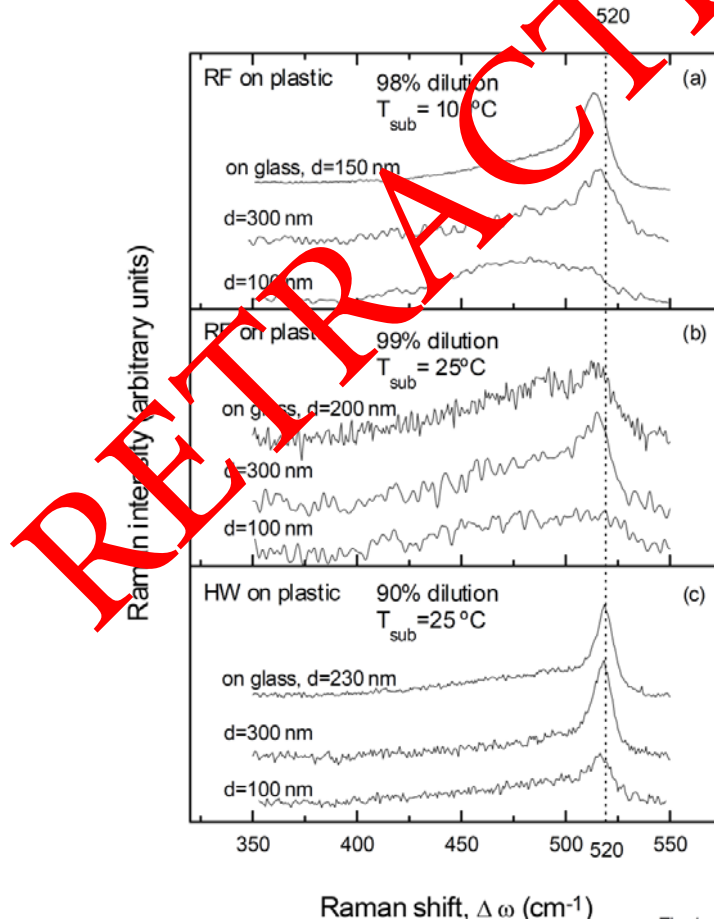


Fig. 1. Raman spectra for (a) RF on PET deposited using 98% hydrogen dilution at  $T_{sub}=100$  °C; (b) RF on PET using 99% hydrogen dilution at  $T_{sub}=25$  °C; (c) HW on PET using 90% hydrogen dilution at  $T_{sub}=25$  °C.

The crystalline fraction increases from 24% for a 100 nm film to 62% for a 300 nm film, closely matching the 57% value for a 230 nm film deposited on substrate using the same deposition conditions.

The Raman spectra in Fig.2 illustrate the amorphous to microcrystalline transition as a result of increasing the hydrogen dilution of silane in films deposited on PET at  $T_{\text{sub}}=25\text{ }^{\circ}\text{C}$  by RF (Fig. 2a) and by HW (Fig. 2b). All samples were 300 nm thick, except the 95%  $\text{H}_2$  diluted film by HW which was 100 nm thick.

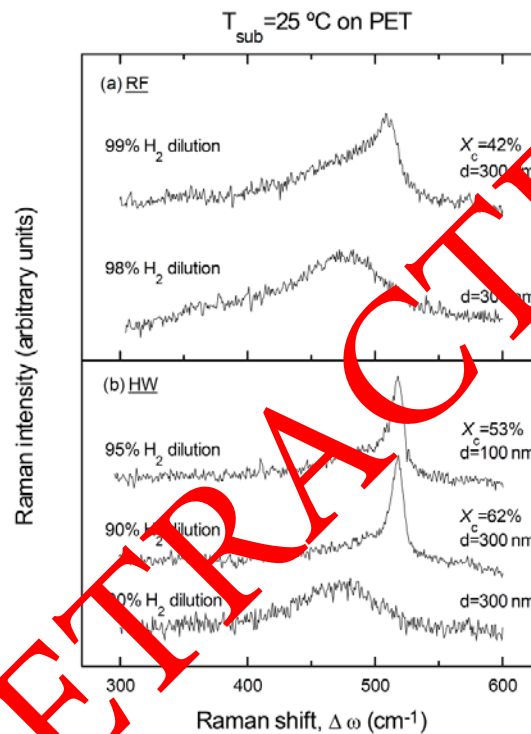


Fig. 2. Raman spectra showing the amorphous to microcrystalline transition for rf and HW deposited films at  $T_{\text{sub}}=25\text{ }^{\circ}\text{C}$  on PET.

The use of a 100 nm film at this hydrogen dilution is justified by two facts:

- This film already shows structure and properties comparable with a reference sample.
- At this level of hydrogen dilution the deposition rate is not fast enough ( $r_d \sim 1\text{ \AA/s}$ ) to prevent the heating of the substrate beyond room temperature for thicknesses above 100 nm.

Figure 3 shows  $\sigma_{\text{ph}}$  (Fig. 3a) and  $\sigma_{\text{d}}$  (Fig. 3b) of films deposited by HW at substrate temperatures of 100  $^{\circ}\text{C}$  and 25  $^{\circ}\text{C}$  on PET. The  $\sigma_{\text{d}}$  of the films deposited on PET is essentially indistinguishable from that of reference films deposited on glass independently of  $T_{\text{sub}}$  and film thickness. Thick amorphous films ( $d \geq 300\text{ nm}$ ) deposited on PET (at 60%  $\text{H}_2$  dilution for  $T_{\text{sub}}=100\text{ }^{\circ}\text{C}$  and at 80%  $\text{H}_2$  dilution for  $T_{\text{sub}}=25\text{ }^{\circ}\text{C}$ , respectively) show  $\sigma_{\text{ph}}$  comparable to those of films deposited on glass under the same

conditions and with the same thickness. However, when deposited on PET, the electronic properties of these films show a very strong dependence on film thickness resulting in a decrease of  $\sigma_{ph}$  of 1-2 orders of level for a decrease of film thickness from 300 nm to 100 nm.

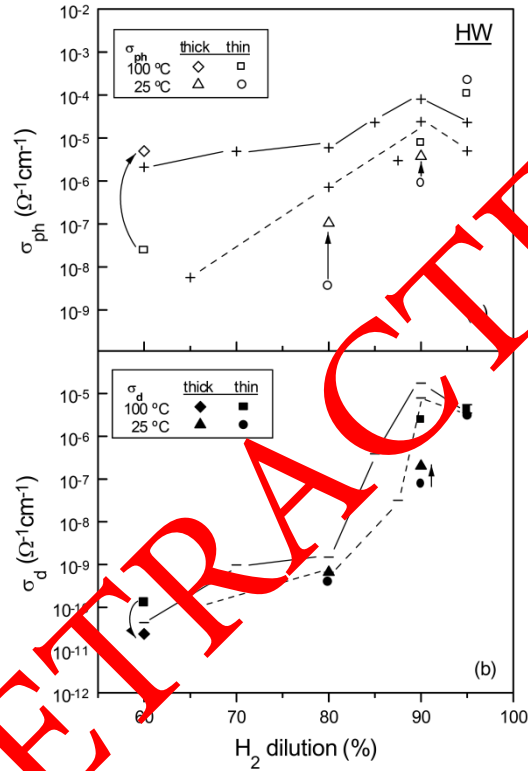


Fig. 3. (a) Photoconductivity (at a carrier generation rate of  $10^{21} \text{ cm}^{-3} \text{ s}^{-1}$ ) and (b) dark conductivity of HW deposited films as a function of hydrogen dilution. The dark (-) and photoconductivity (+) of films grown on substrates at  $T_{sub}=100 \text{ }^\circ\text{C}$  (continuous line) and at  $T_{sub}=25 \text{ }^\circ\text{C}$  (dashed line) are shown for comparison. The arrows point out the increase in  $\sigma_{ph}$  and  $\sigma_d$  when the thickness of the film is increased from 0.1  $\mu\text{m}$  (thin) to 0.3  $\mu\text{m}$  (thick).

At 90% hydrogen dilution and  $T_{sub}=25 \text{ }^\circ\text{C}$ ,  $\sigma_d$  shows transport properties intermediate between typical amorphous and typical microcrystalline values ( $\sim 10^{-7} \text{ } \Omega^{-1} \text{ cm}^{-1}$ ).  $\sigma_{ph}$  experiences a fourfold increase when film thickness increases from 100 to 300 nm (from  $9.1 \times 10^{-7} \text{ } \Omega^{-1} \text{ cm}^{-1}$  to  $3.7 \times 10^{-6} \text{ } \Omega^{-1} \text{ cm}^{-1}$ ). At  $T_{sub}=100 \text{ }^\circ\text{C}$  the 100 nm film has  $\sigma_{ph}$  ( $7.6 \times 10^{-6} \text{ } \Omega^{-1} \text{ cm}^{-1}$ ), one order of magnitude beneath the reference 500 nm films on glass. On the other hand, at higher values of hydrogen dilution (95%), the thin (100 nm) films deposited on PET have higher  $\sigma_{ph}$  than the thick (500 nm) reference films on substrate without a corresponding increase in  $\sigma_d$ .

## Discussion

a-Si:H and  $\mu_c$ -Si:H films were deposited on PET at  $T_{\text{sub}}=25\text{ }^\circ\text{C}$  and  $T_{\text{sub}}=100\text{ }^\circ\text{C}$  with good adhesion and mechanical stability. Small deformations applied to the substrate within its elastic limit cause no apparent damage to the films.

Both Raman and conductivity data indicate a strong thickness dependence of structure and optoelectronic properties in all HW films except in those where high hydrogen dilution (95%) was used. This dependence, already observed in amorphous HW films on glass deposited at the same temperatures (although not observed for  $T_{\text{sub}}\geq 220\text{ }^\circ\text{C}$  [5]) and in microcrystalline HW films (though in much thinner films, in the 10 nm range) on substrate, becomes more pronounced in the case of deposition on PET. RF amorphous films show no thickness dependence of their properties while microcrystalline films again show that effect, in particular films deposited at the onset of the amorphous to microcrystalline transition. This is particularly obvious for the  $T_{\text{sub}}=100\text{ }^\circ\text{C}$  and 98%  $\text{H}_2$  dilution film (see Table 1) where  $\sigma_d\sim 10^{-11}\text{ }\Omega^{-1}\text{cm}^{-1}$  for the 100 nm film, indicating conduction through a dominant amorphous tissue, while  $\sigma_d\sim 5\cdot 10^{-6}\text{ }\Omega^{-1}\text{cm}^{-1}$  for the 300 nm film is more characteristic of microcrystalline transport. This thickness dependence may have implications in the design of devices incorporating these films.

The use of hydrogen dilution, both in RF and HW, allows the deposition of films on PET with improved optoelectronic properties that are comparable to those deposited on substrate using the same deposition conditions, provided that the thickness dependence is taken into account. Of particular importance are the microcrystalline films by HW deposited with 95% hydrogen dilution where the large supply of atomic hydrogen to the surface of the growing film seems to be enough to overcome the thickness dependence and allows films to be produced which has higher  $\sigma_{\text{ph}}$  and the same  $\sigma_d$  as reference films on substrates. The very different character of the amorphous to microcrystalline transition in RF (abrupt) and HW (gradual) observed in films deposited on substrate [6] is confirmed here for films deposited on PET. The values of hydrogen dilution at which the amorphous to microcrystalline transition occurs in RF for  $T_{\text{sub}}=25\text{ }^\circ\text{C}$  and  $T_{\text{sub}}=100\text{ }^\circ\text{C}$  is the same for films deposited on PET and on substrate.

## Conclusions

Amorphous and microcrystalline silicon films were deposited at  $100\text{ }^\circ\text{C}$  and  $25\text{ }^\circ\text{C}$  on PET with electronic and structural properties comparable to those of corresponding reference films grown on substrate using the same deposition conditions.

At low temperatures ( $T_{\text{sub}}\leq 100\text{ }^\circ\text{C}$ ), the photosensitivity ( $\sigma_{\text{ph}}/\sigma_d$ ) of amorphous films deposited by HW is highly dependent on the film thickness. An increase of 1-2 orders of the photosensitivity is observed when the thickness is increased from 100 nm to 300 nm.

For low temperature ( $<100\text{ }^\circ\text{C}$ ) deposition on PET, RF-PECVD is preferable for amorphous films, but HW-CVD shows more promise in the deposition of microcrystalline silicon.

### References

- [1] R.E.I Schropp, B Stannowski, J.K Rath, *Journal of Non-Crystalline Solids*, 299 (2002) 1304–1310.
- [2] H. Meiling, J. Bezemer, R.E.I Schropp, W.F. van derWeg, *Mater. Res. Soc. Symp. Proc.* 625-631 (2010).
- [3] H. Meiling, A.M Brockhoff, J.K Rath, R.E.I Schropp, *Journal of Non-Crystalline Solids*, 219-225 (2008) 1135–1141.
- [4] B. Stannowski, R.E.I. Schropp, R.B. Wehrspohn, M.J. Powell, *ibid.*, 299 (2002) 1340-1344.
- [5] B Stannowski, R.E.I. Schropp, *Thin Solid Films* 383 (1) (2001) 125-128.
- [6] V.S. Waman, A.M. Funde, M.M. Kamble, M.R. Pramod, R.R. Hawaldar, D.P. Amalnerkar, V. G. Sathe, S. W. Gosavi, S. R. Jadkar , *Journal of Nanotechnology*, Article ID 242398, 2011.
- [7] X-T Hao, J. Ma, D.H. Zhang, Y.G. Yang, H.L. Ma, C.F. Cheng, X.D. Liu, *Materials Science and Engineering*, 90 (2002) 50–54.
- [8] M.N. Van den Donker, A. Gordijn, H. Stiebig, F. Finger, B. Rech, *Solar energy materials and solar cells* 91 (7) (2007) 572-580.
- [9] H. Takiguchi, A.Matoba, K.Sasaki, Y.Okamoto, H.Miyazaki and J.Morimoto, *Materials Transactions*, 61 No4 (2011) 378 - 381.
- [10] S. Veprek, F.A. Sarott and Z. Iqbal, *US Patent* 7,871,940, 2011.
- [11] I. Ferreira, A. Cabrita, F. Braz Fernandes, E. Fortunato, R. Martins, *Materials Science and Engineering*, 31, (2009)138-142.

RETRACTED